ELSEVIER

Sensors and Actuators 78 (1999) 180–188

SENSORS AND ACTUATORS A PHYSICAL

www.elsevier.nl/locate/sna

Carbon fiber structural composites as thermistors

Sihai Wen, Shoukai Wang, D.D.L. Chung *

Composite Materials Research Laboratory, State University of New York at Buffalo, Buffalo, NY 14260-4400, USA

Received 18 January 1999; received in revised form 1 June 1999; accepted 4 June 1999

Abstract

Carbon fiber structural composites, in the form of short-fiber silica fume cement–matrix composite and crossply continuous-fiber polymer–matrix composite, were found to be thermistors due to the decrease in electrical resistivity with increasing temperature. The resistivity is the volume resistivity for the cement–matrix composite and the contact resistivity between crossply laminae for the polymer–matrix composite. The activation energy of electrical conduction is up to 0.41 and 0.12 eV for cement–matrix and polymer–matrix composites, respectively. For the polymer–matrix composite, each junction between crossply fiber groups of adjacent laminae is a thermistor, while the fiber groups serve as electrical leads.

Keywords: Composite; Carbon fiber; Cement; Polymer; Thermistor; Temperature sensor

1. Introduction

An NTC thermistor is a thermometric device consisting of a material (typically a semiconductor) whose electrical resistivity decreases with increasing temperature. It is different from thermocouples, which are based on the Seebeck effect. Both thermistors and thermocouples are widely used for temperature sensing.

As the temperature affects the performance, operation and safety of structures, it is valuable to monitor the temperature of a structure. This monitoring is conventionally done by using embedded or attached temperature sensors.

This paper provides a new class of thermistors, which involve carbon fiber structural composites instead of semiconductors. The advantages of the composites are low cost, mechanical ruggedness and processability into various shapes and sizes (as small as a coin or as large as a bridge). The processability into large sizes means that a composite structure is inherently able to sense its own temperature, without the need for embedded or attached sensors. This makes the structure intrinsically smart. Compared to the use of embedded or attached sensors, the intrinsically smart structure has the advantages of low cost, high durability, large sensing volume (everywhere rather than just here and there) and absence of mechanical property degradation (which occurs in the case of embedded sensors).

Concrete is a cement–matrix composite that is important for civil structures. The addition of short fibers as an admixture is known to decrease the drying shrinkage and increase the flexural toughness [1–6]. In the case of the fibers being carbon fibers, the fiber addition also increases the flexural strength and renders the composite the ability to sense its own strain [7–11]. The strain-sensing ability is due to the effect of strain on the volume electrical resistivity of the composite. The Seebeck effect has been reported in carbon fiber cement–matrix composites [12]; it allows the cement–matrix composites to serve as temperature sensors. However, the use of the Seebeck effect for temperature measurement requires Seebeck voltage measurement, such that the voltage drops in the electrical leads and other parts of the circuit are not included. This requirement makes it more complicated to make use of the Seebeck effect in a structure in practice than the thermistor effect (i.e., the decrease of the resistivity with increasing temperature), which relates to resistance measurement rather than voltage measurement. The thermistor effect has not been previously reported in cement–matrix composites, although studies of the electrical resistivity have been made [13–17].

Continuous carbon fiber polymer–matrix composites are widely used for lightweight structures, such as aircraft, sporting goods and even automobiles and wheel chairs. Continuous fibers are not used in cement–matrix compos-

* Corresponding author. Tel.: +1-716-645-2593 ext. 2243; fax: +1-716-645-3875; E-mail: ddlchung@acsu.buffalo.edu

0924-4247/99/$ - see front matter
PII: S0924-4247(99)00240-X

ites due to the high cost of continuous fibers compared to short fibers, the impossibility of having continuous fibers in a concrete mix, and the importance of low cost for a concrete to be industrially viable. For polymer–matrix structural composites, continuous fibers rather than short fibers are used, because continuous fibers are much more effective for reinforcing than short fibers. The thermistor effect has been previously reported in short-fiber polymer–matrix composites [18], but not in continuous-fiber polymer–matrix composites.

The thermistor effect is not only useful for application in temperature-sensing, it is relevant to the study of the electrical conduction mechanism, which relates to the structure of the composite. The sensitivity of a thermistor for temperature-sensing is described by the activation energy of the electrical conduction, as obtained from the negative slope of the Arrhenius plot of the logarithm of the electrical conductivity vs. the reciprocal of the absolute temperature. The activation energy reflects the energy for the hopping of the charge carrier in the composite.

This paper describes the thermistor effect in short carbon fiber cement–matrix composite and continuous carbon fiber polymer–matrix composite. The former was found to be associated with an activation energy that is similar to the values for semiconductors, whereas the latter was found to be associated with a lower activation energy. Hence, the former is superior to the latter for thermistor application. However, the latter is more amenable to practical implementation, because the continuous fibers serve as electrical leads, so that both thermistors and leads are built-in to a continuous fiber composite.

For both carbon fiber polymer–matrix and cement–matrix composites, the electrical resistivity is affected by both temperature and strain. Thus, practical application of these composites for temperature-sensing will require compensation for the effect of strain.

2. Short carbon fiber cement–matrix composites

2.1. Experimental methods

The carbon fibers were isotropic pitch-based, unsized, and of length ~ 5 mm, as obtained from Ashland Petroleum (Ashland, KY). The fiber properties are shown in Table 1. No aggregate (fine or coarse) was used.

Table 1
Properties of carbon fibers used in cement–matrix composites

Filament diameter	15 ± 3 μm
Tensile strength	690 MPa
Tensile modulus	48 GPa
Elongation at break	1.4%
Electrical resistivity	3.0×10^{-3} Ω cm
Specific gravity	1.6 g cm^{-3}
Carbon content	98 wt.%

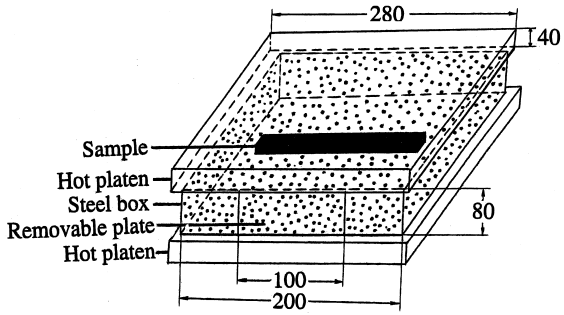

Fig. 1. Experimental set-up for measuring the temperature dependence of the electrical resistivity at and above room temperature. Dimensions are in millimeters.

The cement used was portland cement (Type I) from Lafarge (Southfield, MI). The silica fume (Elkem Materials, Pittsburgh, PA, EMS 965) was used in the amount of 15% by weight of cement. The methylcellulose, used in the amount of 0.4% by weight of cement, was from Dow Chemical, Midland, MI, Methocel A15-LV. The defoamer (Colloids, Marietta, GA, 1010) used whenever methylcellulose was used was in the amount of 0.13 vol%. The latex, used in the amount of 20% by weight of cement, was a styrene butadiene polymer (Dow Chemical, Midland, MI, 460NA) with the polymer making up about 48% of the dispersion and with styrene and butadiene in the weight ratio 66:34, such that the latex was used along with an antifoam (Dow Corning, Midland, MI, no. 2210, 0.5% by weight of latex).

A rotary mixer with a flat beater was used for mixing. Methylcellulose (if applicable) was dissolved in water and then the defoamer was added and stirred by hand for about 2 min. Latex (if applicable) was mixed with the antifoam by hand for about 1 min. Then the methylcellulose mixture (if applicable), the latex mixture (if applicable), cement, water, silica fume (if applicable) and fibers (if applicable) were mixed in the mixer for 5 min. After pouring into molds, an external vibrator was used to facilitate compaction and decrease the amount of air bubbles. The samples were demolded after 24 h and then cured in air at room temperature and a relative humidity of 100% for 28 days.

Five types of cement pastes were studied, namely, (i) plain cement paste (consisting of just cement and water), (ii) silica fume cement paste (consisting of cement, water and silica fume), (iii) carbon fiber silica fume cement paste (consisting of cement, water, silica fume, methylcellulose, defoamer and carbon fibers), (iv) latex cement paste (consisting of cement, water and latex), and (v) carbon fiber latex cement paste (consisting of cement, water, latex and carbon fibers). The water/cement ratio was 0.45 for pastes (i), (ii) and (iii), and was 0.25 for pastes (iv) and (v).

Electrical resistivity measurements were conducted using the two-probe method, with silver paint in conjunction with copper wires for electrical contacts. The two-probe method gave essentially the same result as the four-probe

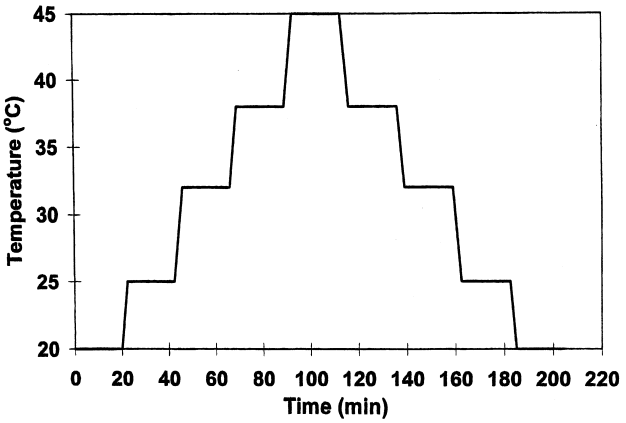

Fig. 2. Temperature vs. time during stepped heating and cooling.

method, due to the high sample resistance. A Keithley 2001 multimeter was used. Samples were in the form of rectangular bars of size 150 mm × 12 mm × 11 mm. Each electrical contact was applied around the entire 12 mm × 11 mm perimeter of the bar. The two contacts were at two parallel cross-sectional planes that were 40 mm apart. The temperature was varied by putting a sample in a steel open box (200 mm × 200 mm × 80 mm) which was sandwiched by hot platens (280 mm × 280 mm) that were resistance-heated (Fig. 1). The sample was electrically insulated from the steel box and did not touch either platen. The temperature of the sample was measured by using a thermocouple which touched the middle of the top surface of the sample. A removable plate (100 mm × 80 mm) at a side of the steel box allowed electrical leads from the sample to come out. The temperature was raised and then lowered in steps between 20° and 45°C (Fig. 2). Current–voltage characteristic measurement was made at each step. Six samples of each of the five types of paste were tested.

For paste (iii) alone, electrical resistivity measurement was also conducted below room temperature by putting the sample in a freezer with temperature control. No box was used to house the sample, in contrast to measurements above room temperature. The temperature was measured by using a thermocouple which touched the middle of the top surface of the sample. It was raised in steps from 1° to 7°C and then to 14°C, and then lowered in steps to 7°C and then to 1°C. The steady-state time at each step was 20 min, as in Fig. 2. Six samples of paste (iii) were tested.

Table 2
Resistivity and critical voltage of carbon fiber silica fume cement paste

Temperature (°C) during stepped heating and cooling	Resistivity (10^4 Ω cm)	Critical voltage (V)
20	1.73 ± 0.08	8.15 ± 0.34
25	1.38 ± 0.12	6.82 ± 0.47
32	0.90 ± 0.14	5.76 ± 0.52
38	0.69 ± 0.09	5.07 ± 0.39
45	0.44 ± 0.09	4.24 ± 0.43
38	0.76 ± 0.13	5.51 ± 0.38
32	1.01 ± 0.09	6.44 ± 0.56
25	1.50 ± 0.16	7.41 ± 0.49
20	1.92 ± 0.18	9.05 ± 0.66
1	4.47 ± 0.24	10.30 ± 0.21
7	3.36 ± 0.31	9.76 ± 0.30
14	2.13 ± 0.15	9.14 ± 0.32
7	3.80 ± 0.19	10.10 ± 0.36
1	5.28 ± 0.36	10.70 ± 0.27

2.2. Results

Fig. 3 shows the current–voltage characteristic of carbon fiber silica fume cement paste at 38°C during stepped heating. The characteristic is linear below 5 V and deviates positively from linearity beyond 5 V. The resistivity is obtained from the slope of the linear portion. The voltage, at which the characteristic starts to deviate from linearity, is hereby referred to as the critical voltage. The shape of the characteristic is similar for all samples at all temperatures, though the values of the resistivity and critical voltage differ, as listed in Table 2.

Fig. 4 shows a plot of resistivity vs. temperature during heating and cooling for carbon fiber silica fume cement

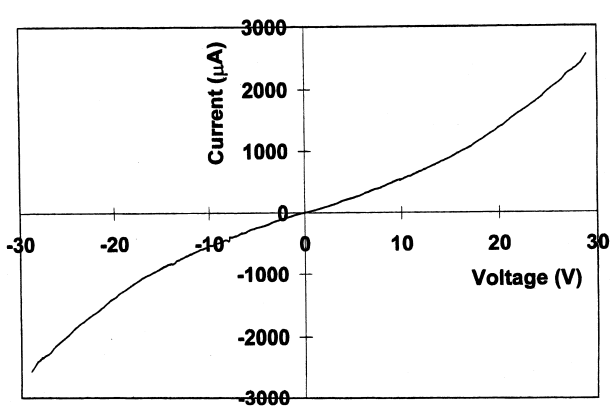

Fig. 3. Current–voltage characteristic of carbon fiber silica fume cement paste at 38°C during stepped heating.

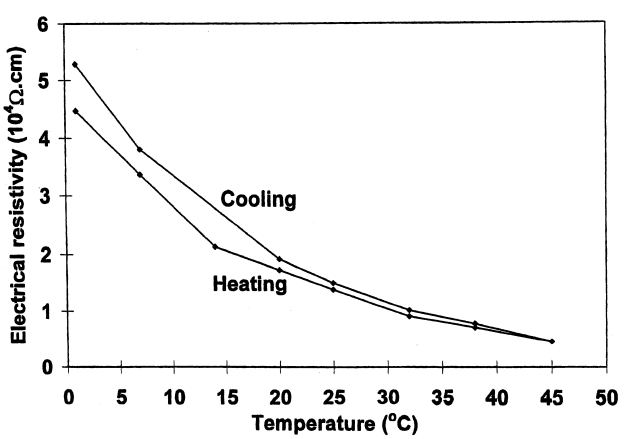

Fig. 4. Plot of electrical resistivity vs. temperature during heating and cooling for carbon fiber silica fume cement paste.

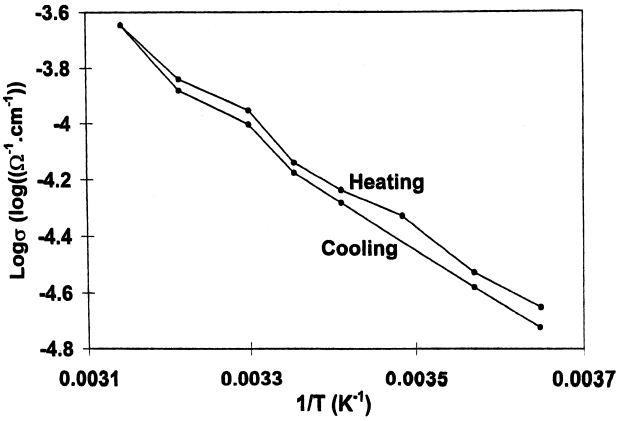

Fig. 5. Arrhenius plot of log electrical conductivity vs. reciprocal absolute temperature for carbon fiber silica fume cement paste.

paste. The resistivity decreased upon heating and the effect was quite reversible upon cooling. That the resistivity was slightly increased after a heating–cooling cycle is probably due to thermal degradation of the material. Fig. 5 shows the Arrhenius plot of log conductivity (conductivity = 1/resistivity) vs. reciprocal absolute temperature. The slope of the plot gives the activation energy, which is 0.390 ± 0.014 and 0.412 ± 0.017 eV during heating and cooling, respectively. Fig. 6 shows a plot of the critical voltage vs. temperature during heating and cooling. The critical voltage decreased upon heating and the effect was reversible upon cooling. That the critical voltage was slightly increased after a heating–cooling cycle is probably due to thermal degradation of the material.

Results similar to those of carbon fiber silica fume cement paste were obtained with the remaining types of cement paste, i.e., carbon fiber latex cement paste, silica fume cement paste, latex cement paste and plain cement paste, except that, for all the remaining four types of cement paste, (i) the resistivity was higher by about an order of magnitude, and (ii) the activation energy was lower by about an order of magnitude, as shown in Table 3. The critical voltage was higher when fibers were absent (Table 3).

2.3. Discussion

Comparison between carbon fiber silica fume cement paste and silica fume cement paste shows that the presence of carbon fibers decreases the electrical resistivity and causes the resistivity to decrease with increasing temperature more significantly, as indicated by a higher activation energy, which is desirable for thermistors. The low resistivity when fibers are present is due to the high conductivity of the fibers compared to the cement matrix. The high activation energy when fibers are present is due to the hopping conduction between cement matrix and fiber. Note that the fiber volume fraction is below the percolation threshold [1], so that direct hopping from fiber to fiber is relatively insignificant. In the absence of fibers, the activation energy is low, because the interfaces in silica fume cement paste are relatively diffuse and hopping across them does not require much energy.

Comparison of latex cement paste and carbon fiber latex cement paste shows that the resistivity is decreased by the fiber addition, but the extent of the decrease is much less than that in the case of adding fibers to silica fume cement paste. Moreover, adding fibers to latex cement paste does not affect the activation energy, in contrast to the large increase in activation energy upon adding fibers to silica fume cement paste. Comparison of carbon fiber silica fume cement paste and carbon fiber latex cement paste shows that the replacement of silica fume with latex increases the resistivity and decreases the activation energy to values below those of plain cement paste. These characteristics are attributed to the lower ability of latex compared to silica fume for dispersing the fibers [19] and the electrical insulation ability of latex, which resides at the fiber–matrix interface [20]. Hence, like cement pastes without carbon fibers, carbon fiber latex cement paste is not attractive for use as thermistors.

The activation energy for hopping from carbon fiber to carbon fiber in a polymer–matrix composite ranges from 0.01 to 0.1 eV (Section 3). The polymer matrix is not conducting, so hopping from fiber to fiber is necessary. However, the cement matrix is conducting, so hopping between fiber and cement paste is sufficient for conduction. It appears that hopping between fiber and cement matrix (without latex but with silica fume) requires more energy than hopping from fiber to fiber. This is reasonable due to the weak bond between carbon fiber and the cement matrix [21,22]. Hence, carbon fiber silica fume cement–matrix composites are more attractive than carbon fiber polymer–matrix composites for use as thermistors. The cement–matrix composites are not as attractive as silicon (a semiconductor), which has an activation energy of 0.56 eV (half of the energy band gap), but are more attractive than germanium (a semiconductor), which has an activa-

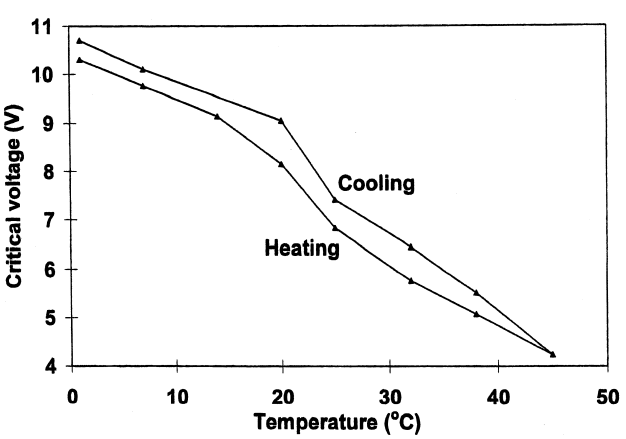

Fig. 6. Plot of the critical voltage vs. temperature during heating and cooling for carbon fiber silica fume cement paste.

Table 3
Resistivity, critical voltage and activation energy of five types of cement paste

Formulation	Resistivity at 20°C (Ω cm)	Critical voltage at 20°C (V)	Activation energy (eV)	
			Heating	Cooling
Plain	$(4.87 \pm 0.37) \times 10^5$	10.80 ± 0.45	0.040 ± 0.006	0.122 ± 0.006
Silica fume	$(6.12 \pm 0.15) \times 10^5$	11.60 ± 0.37	0.035 ± 0.003	0.084 ± 0.004
Carbon fibers + silica fume	$(1.73 \pm 0.08) \times 10^4$	8.15 ± 0.34	0.390 ± 0.014	0.412 ± 0.017
Latex	$(6.99 \pm 0.12) \times 10^5$	11.80 ± 0.31	0.017 ± 0.001	0.025 ± 0.002
Carbon fibers + latex	$(9.64 \pm 0.08) \times 10^4$	8.76 ± 0.35	0.018 ± 0.001	0.027 ± 0.002

tion energy of 0.34 eV. On the other hand, cement–matrix composites are much less expensive than the semiconductors.

Presumably due to thermal degradation, the resistivity of cement–matrix composites is higher during cooling than during the initial heating. As a result, the activation energy is higher during cooling than during heating. For thermistor applications, the behavior during cooling is more relevant, due to its relative stability.

The deviation from linearity of the current–voltage characteristic corresponds to the resistivity decreasing with increasing electric field. This effect is attributed to Joule heating and the decrease of the resistivity with increasing temperature. The critical voltage is lower for cement pastes containing carbon fibers than those without fibers, probably because of the lower resistivity when fibers are present. Carbon fiber silica fume cement paste has lower resistivity and lower critical voltage than carbon fiber latex cement paste.

3. Continuous carbon fiber polymer–matrix composites

The origin of the ability of a continuous carbon fiber polymer–matrix composite for sensing temperature lies in the effect of temperature on the DC contact electrical resistivity of the junction between crossply fiber groups (one or more tows in a group) in two adjacent crossply laminae of the composite. Temperature increase causes this resistivity to decrease reversibly, so that the resistance provides a measure of the temperature. This thermal phenomenon is due to the activation energy for electron jumping from one lamina to the other.

A carbon fiber polymer–matrix composite temperature detector can be in the form of two layers of fibers that are 90° from one another. Each junction of the 0° and 90° fiber groups (multiple tows per group) is an independent detector (Fig. 7). The crossing fiber groups serve as electrical leads for a detector, which is the junction of the crossing fiber groups (Fig. 8). The contact resistivity of each crossing can be best measured by using the four-probe method, in which two probes (A and D) are for passing the current and two probes (B and C) are for measuring the voltage. (The two-probe method is simpler but less accurate; it uses two probes so that the current and voltage probes are not

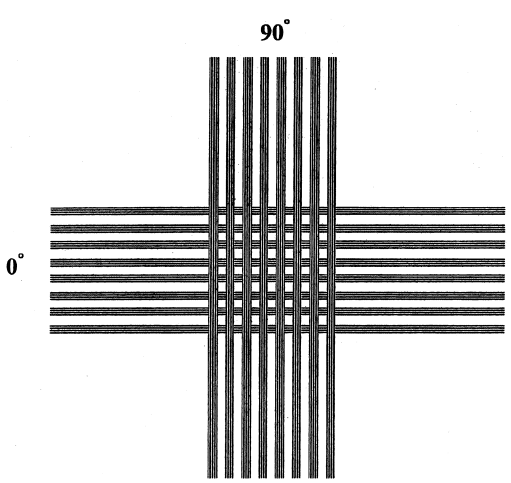

Fig. 7. Temperature sensor array in the form of a carbon fiber polymer–matrix composite comprising two crossply laminae.

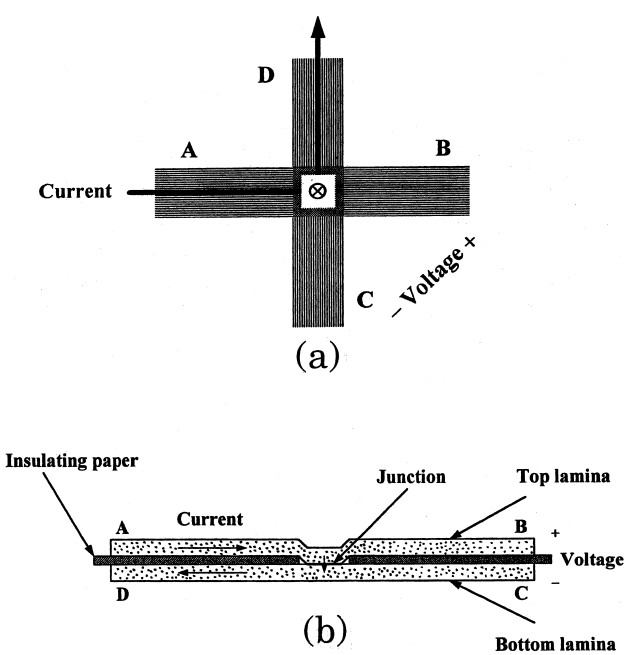

Fig. 8. (a) A single temperature sensor in the form of a junction between two crossply lamina (top view). The contact resistivity of the junction is measured by using current probes A and D and voltage probes B and C. The fibers serve as electrical leads. (b) A junction between two unidirectional laminae (side view). In both (a) and (b), the arrows indicate the current path.

Table 4
Carbon fiber and epoxy matrix properties (according to ICI Fiberite)

10E-Torayca T-300 (6 K) untwisted, UC-309 sized	
Diameter	7 μm
Density	1.76 g cm^{-3}
Electrical resistivity	2.2×10^{-3} Ω cm
Tensile modulus	221 GPa
Tensile strength	3.1 GPa
976 epoxy	
Process temperature	350°F (177°C)
Maximum service temperature	350°F (177°C) dry
	250°F (121°C) wet
Flexural modulus	3.7 GPa
Flexural strength	138 MPa
T_g	232°C
Density	1.28 g cm^{-3}

separate and the contact potential resulting from the contact resistance of each probe is included in the measured voltage.) In the four-probe method, the current flows from current probe A along one fiber group, turns to the through-thickness direction and flows through the crossing from one fiber group to the other; and then turns direction again to flow along the other fiber group towards current probe D. The voltage between probes B and C gives the voltage across the junction. The voltage divided by the current is the resistance of the junction. The resistance multiplied by the junction area is the contact resistivity of the junction. The array of junctions in Fig. 7 allows determination of the location on the composite at which heat is applied. Computer data acquisition allows the contact resistivity of the junctions in the array to be measured one junction at a time, so that the whole array is measured in a reasonably short time. As the fiber groups serve as electrical leads, no wiring is needed. Not all the groups need to serve as leads, because the spatial resolution of the heat detection does not need to be excessive.

The top two fiber layers of a composite structure capable of temperature detection should be crossply (Fig. 7). The layers below can be in other lay-up configurations. The fibers in the top two layers should be longer than those in the other layers in order to facilitate electrical connection.

The fractional change in contact resistivity per degree Celsius is around −0.13% to −1.10% (negative because the resistivity decreases upon heating) for a carbon fiber epoxy–matrix composite, as reported in this paper. The greater is the volume fraction of the fibers, the higher is the interlaminar stress, the greater is the activation energy, and the larger is the magnitude of the fractional change in contact resistivity per degree Celsius.

A thermocouple array can be used to provide spatially resolved temperature detection. However, a thermocouple array requires much wiring. In addition, the thermocouple tips must be at or near the outer surface of the composite structure. If the thermocouples are embedded in the composite, they are intrusive and degrade the mechanical properties of the composite. If the thermocouples are attached on the surface of the composite, they can come off easily. Therefore, in practice, a thermocouple array is not feasible for spatially resolved temperature sensing.

3.1. Experimental methods

Two laminae of unidirectional carbon fiber epoxy–matrix prepregs (Table 4) in the form of strips crossing one another, with one strip on top of the other (Fig. 8), were fabricated into a composite at the overlapping region (6 mm × 6 mm) of the two laminae by applying pressure and heat to the overlapping region (without a mold). The pressure was provided by a weight, which was varied in order to vary the pressure. A glass fiber epoxy–matrix composite spacer was placed between the weight and the junction (the overlapping area region of the two strips). The heat was provided by a Carver hot press. A Watlow model 981C-10CA-ARRR temperature controller was used to control the temperature and the ramping rate. Each of the samples was put between the two heating platens of the hot press and heated linearly up to 175 ± 2°C at the rate of 2.5°C min^{-1}. Then it was cured at that temperature for 10 h and subsequently cooled linearly to 50 ± 2°C at the rate of 0.18°C min^{-1}. After that, the sample was reheated up to 150 ± 2°C and then cooled back to 50 ± 2°C. Both the reheating and the subsequent cooling were linear and at the rate of 0.15°C min^{-1}. After the reheating and cooling, the sample was heated linearly up to 150 ± 2°C again at the rate of 1°C min^{-1} and then cooled linearly back to 50 ± 2°C at the rate of 0.15°C min^{-1}. All the time, the contact electrical resistance and the temperature of the sample were measured, respectively, by a Keithley 2001 multimeter and a T-type thermocouple, which was put just beside the junction. Electrical contacts were made to the four ends

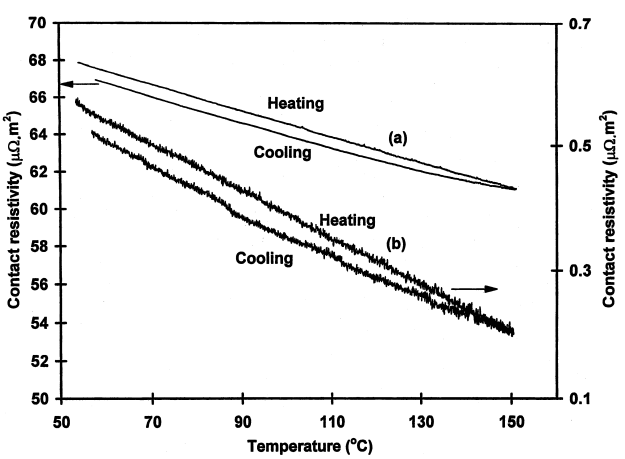

Fig. 9. Variation of contact electrical resistivity with temperature during heating and cooling at 0.15°C min^{-1} (a) for sample made without any curing pressure, and (b) for sample made with a curing pressure 0.33 MPa.

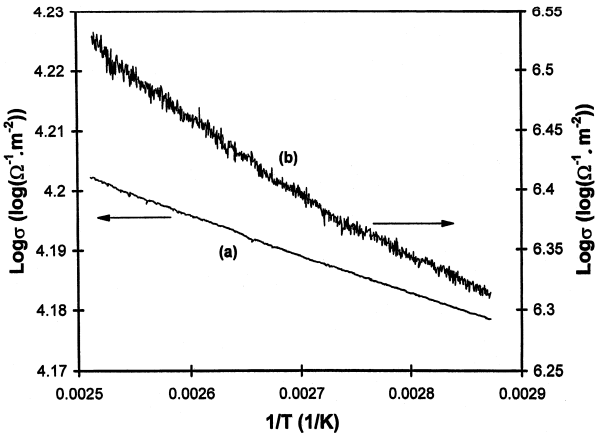

Fig. 10. Arrhenius plot of log contact conductivity vs. inverse absolute temperature during heating at 0.15°C min^{-1} (a) for sample made without any curing pressure, and (b) for sample made with curing pressure 0.33 MPa.

of the two strips, so as to measure the contact electrical resistivity (resistance multiplied by contact area, which is the area of the overlapping region) between the two laminae in the composite, using the four-probe method (Fig. 8). The epoxy at the ends of each prepreg strip was burned out to expose the carbon fibers for the purpose of making electrical contacts. These exposed fibers were wrapped by pieces of copper foil, with silver paint between the copper foil and the fibers. The electric current flowed from A to D, such that the dominant resistance was the contact resistance, as the volume resistance of the strips was negligible in comparison. The voltage between B and C is the voltage between the two laminae.

3.2. Results and discussion

The current–voltage characteristic is linear for all samples studied. Fig. 9 shows the variation of the contact resistivity ρ_c with temperature during reheating and subsequent cooling, both at 0.15°C min^{-1}, for samples cured at 0 and 0.33 MPa. The corresponding Arrhenius plots of log contact conductivity (inverse of contact resistivity) vs. inverse absolute temperature during heating are shown in Fig. 10. From the slope (negative) of the Arrhenius plot, which is quite linear, the activation energy can be calculated. The linearity of the Arrhenius plot means that the activation energy does not change throughout the temperature variation. This activation energy is the energy for electron jumping from one lamina to the other. Electronic excitation across this energy enables conduction in the through-thickness direction. This activation phenomenon is common in the electrical conduction of composite materials with an insulating matrix and an electrically conducting filler (whether particles or fibers). Based on volume resistivity measurement, an activation energy in the range from 0.060 to 0.069 eV has been previously reported for short carbon fiber polymer–matrix composites [18]. Direct measurement of the contact resistivity is impossible for the short-fiber composites.

A slightly concave shape is present in the Arrhenius plots obtained during heating as well as cooling (Fig. 10). This shape means that the activation energy increases slightly with increasing temperature. On the other hand, the interlaminar thermal stress decreases with increasing temperature, as explained in the next paragraph. Thus, this curvature cannot be explained by considering the effect of the thermal stress on the activation energy. The curvature is probably because of the change in the moisture content, which decreases with increasing temperature. Moisture makes the epoxy matrix dilate slightly, thus diminishing the proximity among the fibers and decreasing the contact conductivity of the interface. As a consequence, a moisture content decrease causes the conductivity to increase.

The activation energies, thicknesses and room temperature contact resistivities for samples made at different curing pressures and composite configurations are shown in Table 5. All the activation energies were calculated based on the data at 75°–125°C. In this temperature regime, the temperature change was very linear and well-controlled. From Table 5 it can be seen that, for the same composite configuration (crossply), the higher was the curing pressure, the smaller was the composite thickness (because of more epoxy being squeezed out), the lower was the contact resistivity, and the higher the activation energy. A smaller composite thickness corresponds to a

Table 5
Activation energy for various composites
The standard deviations are shown in parentheses.

Composite configuration	Curing pressure (MPa)	Composite thickness (mm)	Contact resistivity ρ_{co} (Ω cm^2)	Activation energy (eV)		
				Heating at 0.15°C min^{-1}	Heating at 1°C min^{-1}	Cooling at 0.15°C min^{-1}
Crossply	0	0.36	0.73	0.0131 (2×10^{-5})	0.0129 (3×10^{-5})	0.0125 (8×10^{-6})
	0.062	0.32	0.14	0.0131 (4×10^{-5})	0.0127 (7×10^{-5})	0.0127 (4×10^{-5})
	0.13	0.31	0.18	0.0168 (3×10^{-5})	0.0163 (4×10^{-5})	0.0161 (2×10^{-5})
	0.19	0.29	0.054	0.0222 (3×10^{-5})	0.0223 (3×10^{-5})	0.0221 (1×10^{-5})
	0.33	0.26	0.0040	0.118 (4×10^{-4})	0.129 (8×10^{-4})	0.117 (3×10^{-4})
Unidirectional	0.42	0.23	0.29	0.0106 (3×10^{-5})	0.0085 (4×10^{-5})	0.0081 (2×10^{-5})

higher fiber volume fraction in the composite. During curing and subsequent cooling, the matrix shrinks. For carbon fibers, the modulus in the longitudinal direction is much higher than that in the transverse direction. Moreover, the carbon fibers are continuous in the longitudinal direction. Thus, the overall shrinkage in the longitudinal direction tends to be less than that in the transverse direction. In other words, there is CTE difference between the longitudinal and transverse directions and hence, a CTE mismatch between any two crossply layers. Therefore, there will be a residual interlaminar stress in the two crossply layers in a given direction. The stress is compressive in the longitudinal direction and tensile in the transverse direction. This stress accentuates the barrier for the electrons to jump from one lamina to the other. After curing and subsequent cooling, heating will decrease the thermal stress. Both the thermal stress and the curing stress contribute to the residual interlaminar stress. Therefore, the higher the curing pressure, the larger the fiber volume fraction, the greater the CTE mismatch between the crossply laminae, the greater the residual interlaminar stress, and the higher is the activation energy, as shown in Table 5. Besides the residual stress, thermal expansion can also affect the contact resistance by changing the contact area. However, calculation shows that the contribution of thermal expansion is less than one-tenth of the observed change in contact resistance with temperature.

The activation energy increased gradually with increasing curing pressure from 0 to 0.19 MPa, but increased abruptly from 0.02 to 0.12 eV when the curing pressure was increased from 0.19 to 0.33 MPa. The abrupt increase at high pressure is probably not due to the interlaminar stress abruptly increasing, but is probably due to another phenomenon that occurred at the high curing pressure of 0.33 MPa. This phenomenon has not been investigated, but one possibility is that the pressure greatly increased the proximity of the fibers, as suggested by the abrupt drop in contact resistivity when the curing pressure was increased from 0.19 to 0.33 MPa (Table 5). The proximity may allow tunnelling of the electrons across the epoxy between fibers of adjacent laminae, at least at certain points with sufficient proximity. Another possibility is the pressure increasing the anisotropy of the matrix and thereby accentuating the barrier for electron jumping from one lamina to the other.

The curing pressure for the sample in the unidirectional composite configuration was higher than that of any of the crossply samples (Table 5). Consequently, the thickness was the lowest. As a result, the fiber volume fraction was the highest. However, the contact resistivity of the unidirectional sample was the second highest rather than being the lowest, and its activation energy was the lowest rather than the highest. The low activation energy is consistent with the fact that there was no CTE or curing shrinkage mismatch between the two unidirectional laminae and, as a result, no interlaminar stress between the laminae. This low value supports the notion that the interlaminar stress is important in affecting the activation energy. The high contact resistivity for the unidirectional case can be explained in the following way. In the crossply samples, the pressure during curing forced the fibers of the two laminae to press on to one another and hence, contact tightly. In the unidirectional sample, the fibers of one of the laminae just sank into the other lamina at the junction, so pressure helped relatively little in the contact between fibers of adjacent laminae. Moreover, in the crossply situation, every fiber at the lamina–lamina interface contacted many fibers of the other lamina, while, in the unidirectional situation, every fiber had little chance to contact the fibers of the other lamina. Therefore, the number of contact points between the two laminae was less for the unidirectional sample than the crossply samples. Fig. 9 also shows a small irreversible decrease in the room temperature contact resistivity after a heating–cooling cycle. This is mainly due to the decrease in moisture content during heating, as shown by testing specimens having various moisture contents, as attained by allowing the specimens to sit in air for different lengths of time. The irreversibility vanished when the temperature change was small (e.g., temperature changing from 20° to 100°C). The larger the temperature change, the more significant the irreversibility. The slight irreversibility is consistent with the fact that the activation energy obtained during cooling was slightly less than that obtained during heating (Table 5). Table 5 also shows that the heating rate essentially did not affect the activation energy.

4. Conclusion

Carbon fiber silica fume cement paste was found to be an effective thermistor. The electrical resistivity decreased with increasing temperature (1°–45°C), with an activation energy of electrical conduction (electron hopping) of 0.4 eV, which is comparable to those of semiconductors (typical thermistor materials) and higher than that of carbon fiber polymer–matrix composites. Without carbon fibers, or with latex in place of silica fume, the activation energy is much lower and the resistivity is higher. The voltage range for linear current–voltage characteristic is narrower when fibers are present than when fibers are absent. Linearity occurred up to 8 V for carbon fiber silica fume cement paste at 20°C.

An epoxy–matrix continuous carbon fiber composite comprising two crossply laminae was a thermistor array. Each junction between crossply fiber tow groups of the adjacent laminae was a thermistor, while the fiber groups served as electrical leads. The contact electrical resistivity of the junction decreased reversibly upon heating, due to the electron hopping between the laminae. The fractional change in contact resistivity provided an indication of temperature. The contact resistivity decreased with increas-

ing pressure during composite fabrication, due to increase in pressure exerted by fibers of one lamina on those of the other lamina. The magnitude of the fractional change in contact resistivity per degree Celsius increased with increasing curing pressure (fiber volume fraction), due to the increase in interlaminar stress with increasing fiber volume fraction and the consequent increase in activation energy. A crossply junction is much better than a unidirectional junction as a thermistor, due to the absence of interlaminar stress in the latter.

Acknowledgements

This work was supported, in part, by the National Science Foundation. Technical assistance by Mr. Zeng-Qiang Shi of State University of New York at Buffalo is acknowledged.

References

[1] P.-W. Chen, D.D.L. Chung, Low-drying shrinkage concrete containing carbon fibers, Composites, Part B 27B (1996) 269–274.
[2] P.-W. Chen, D.D.L. Chung, A comparative study of concretes reinforced with carbon, polyethylene and steel fibers and their improvement by latex addition, ACI Mater. J. 93 (2) (1996) 129–133.
[3] N. Banthia, Carbon fiber cements: Structure, Performance, Applications and Research Needs, in: J.I. Daniel, S.P. Shah (Eds.), Fiber-Reinforced Concrete, ACI SP-142, ACI Detroit, MI, 1994, pp. 91–119.
[4] H.A. Toutanji, T. El-Korchi, R.N. Katz, Strength and reliability of carbon fiber-reinforced cement composites, Cem. Concr. Compos. 16 (1994) 15–21.
[5] P. Soroushian, M. Nagi, J. Hsu, Optimization of the use of lightweight aggregates in carbon fiber reinforced cement, ACI Mater. J. 89 (3) (1992) 267–276.
[6] H. Sakai, K. Takahashi, Y. Mitsui, T. Ando, M. Awata, T. Hoshijima, Flexural behavior of carbon fiber-reinforced cement composite, in: J.I. Daniel, S.P. Shah (Eds.), Fiber-Reinforced Concrete, ACI SP-142, ACI, Detroit, MI, 1994, pp. 121–140.
[7] P.-W. Chen, D.D.L. Chung, Concrete as a new strain/stress sensor, Composites, Part B 27B (1996) 11–23.
[8] D.D.L. Chung, Strain sensors based on the electrical resistance change accompanying the reversible pull-out of conducting short fibers in a less conducting matrix, Smart Mater. Struct. 4 (1995) 59–61.
[9] X. Fu, W. Lu, D.D.L. Chung, Improving the strain-sensing ability of carbon fiber-reinforced cement by ozone treatment of the fibers, Cem. Concr. Res. 28 (2) (1998) 183–187.
[10] X. Fu, D.D.L. Chung, Effect of curing age on the self-monitoring behavior of carbon fiber-reinforced mortar, Cem. Concr. Res. 27 (9) (1997) 1313–1318.
[11] X. Fu, E. Ma, D.D.L. Chung, W.A. Anderson, Self-monitoring in carbon fiber-reinforced mortar by reactance measurement, Cem. Concr. Res. 27 (6) (1997) 845–852.
[12] M. Sun, Z. Li, Q. Mao, D. Shen, Study on the hole conduction phenomenon in carbon fiber-reinforced concrete, Cem. Concr. Res. 28 (4) (1998) 549–554.
[13] P.-W. Chen, D.D.L. Chung, Improving the electrical conductivity of composites comprised of short conducting fibers in a non-conducting matrix: the addition of a non-conducting particulate filler, J. Electron. Mater. 24 (1) (1995) 47–51.
[14] P. Xie, P. Gu, J.J. Beaudoin, Electrical percolation phenomena in cement composites containing conductive fibers, J. Mater. Sci. 31 (15) (1996) 4093–4097.
[15] N. Banthia, S. Djeridane, M. Pigeon, Electrical resistivity of carbon and steel microfiber-reinforced cements, Cem. Concr. Res. 22 (1992) 804–814.
[16] X. Ping, J.J. Beaudoin, Characterization of cement–aggregate interfaces by electrical conductivity methods, Proc. Engineering Foundation Conference, Cement Manufacture and Use, ASCE, 1994, pp. 15–25.
[17] P.-W. Chen, D.D.L. Chung, Concrete reinforced with up to 0.2 vol% of short carbon fibers, Composites 24 (1) (1993) 33–52.
[18] A.R. Blythe, Electrical Properties of Polymers, Cambridge Univ. Press, Cambridge, 1980.
[19] P.-W. Chen, X. Fu, D.D.L. Chung, Microstructural and mechanical effects of latex, methylcellulose and silica fume on carbon fiber-reinforced cement, ACI Mater. J. 94 (2) (1997) 147–155.
[20] X. Fu, D.D.L. Chung, Effects of water–cement ratio, curing age, silica fume, polymer admixtures, steel surface treatments, and corrosion on bond between concrete and steel reinforcing bars, ACI Mater. J. 95 (6) (1998) 725–734.
[21] X. Fu, D.D.L. Chung, Contact electrical resistivity between cement and carbon fiber: its decrease with increasing bond strength and its increase during fiber pull-out, Cem. Concr. Res. 25 (7) (1995) 1391–1396.
[22] X. Fu, W. Lu, D.D.L. Chung, Improving the bond strength between carbon fiber and cement by fiber surface treatment and polymer addition to cement mix, Cem. Concr. Res. 26 (7) (1996) 1007–1012.

Sihai Wen is a PhD graduate student of the Department of Mechanical and Aerospace Engineering, State University of New York at Buffalo, and received an MS degree in Materials Engineering from South China University of Technology, China, in 1995.

Shoukai Wang is a PhD graduate student of the Department of Mechanical and Aerospace Engineering, State University of New York at Buffalo, and received an ME degree in Materials Science and Engineering from Beijing University of Aeronautics and Astronautics, China, in 1985.

D.D.L. Chung is a Professor of Mechanical and Aerospace Engineering, the Niagara Mohawk Power Endowed Chair of Materials Research, and the Director of Composite Materials Research Laboratory, at State University of New York at Buffalo, and received a PhD in Materials Science from Massachusetts Institute of Technology in 1977.